SIMPLIFIED PROCEDURE FOR SEISMIC EVALUATION OF PILES WITH PARTIAL-MOMENT-CONNECTION TO THE DECK IN MARINE OIL TERMINALS

By

Rakesh K. Goel[1], F.ASCE

ABSTRACT

This paper presents development of a simplified procedure for seismic evaluation of piles with partial-moment-connection typically used in marine oil terminals. The current seismic evaluation procedure of the piles in marine oil terminals includes monitoring material strains specified in the Marine Oil Terminal Engineering and Maintenance Standard (MOTEMS) during the nonlinear static pushover analysis to estimate the displacement capacity of piles. This investigation developed closed-form formulas for estimating the displacement capacity of piles by utilizing a simple pile-deck connection system. The displacement capacity estimated from these formulas ensures that the material stain limits specified in the MOTEMS is not exceeded. These formulas are demonstrated to be "accurate" by comparing results from these formulas against those from the nonlinear finite-element analysis. The formulas developed in this investigation utilize the curvature ductility capacity of the pile section and rotation ductility capacity of the connection at the selected seismic design level, along with the parameter β which depends on the relative stiffness of the pile and the connection and the parameter η which depends on the relative strength of the connection and the pile.

KEY-WORDS

Marine terminals, Nonlinear analysis, Piers, Piles, Seismic analysis, Seismic design

[1] Professor, Department of Civil & Environmental Engineering, California Polytechnic State University, San Luis Obispo, CA 93407-0353. Email: rgoel@calpoly.edu

INTRODUCTION

Marine oil terminals employ vertical piles to resist gravity loads as well as seismic loads. While the gravity load piles may be connected to the deck by a pin-connection, seismic load piles are typically connected to the deck by a partial-moment-connection. The connection is designed such that its moment capacity is smaller than the moment capacity of the pile. As a result, the yielding is expected to occur in the connection rather than the pile. The nonlinear behavior of piles with such partial-moment-connection to the deck slab may differ significantly from those of piles in which the connection is stronger than the pile and as a result yielding occurs in the pile and not the connection. This paper investigates seismic behavior of two types of piles commonly used in marine oil terminals with partial-moment-connection – hollow-steel piles connected to the deck by a concrete plug and dowels, and pre-stressed-concrete piles connected to the deck by dowels grouted into sleeves in the pile.

Figure 1a shows details of the typical connection between hollow-steel pile and concrete deck of marine oil terminals (Ferrito et al., 1999; Nezamian et al., 2006). In this connection, denoted as the concrete-plug connection, dowels are embedded in a concrete-plug at the top of the pile. The concrete-plug is held in place by shear rings at its top and bottom; the shear rings would prevent the concrete plug from slipping out (or popping-out) during lateral loads imposed by earthquakes. Others have proposed details in which the concrete-plug is held in place either by natural roughness of the inside surface of the steel shell or use of weld-metal laid on the inside of the steel shell in a continuous spiral in the connection region prior to placing the concrete plug (Ferritto et al., 1999). The dowels are then embedded in the concrete deck to provide sufficient development length. A small gap may or may not be provided between top of the pile and top of the concrete-plug. This concrete-plug connection in hollow-steel piles has been shown to provide remarkable ductility (Priestley and Park, 1984; Park et al., 1987).

Figure 1b shows details of the connections between pre-stressed-concrete pile and concrete deck of marine oil terminals (Klusmeyer and Harn, 2004; Roeder et al., 2005; Restrepo et al., 2007; Wray et al., 2007). Pre-stressed-concrete piles typically have corrugated metal sleeves that are embedded in the concrete. These sleeves are located inside of the confined concrete core formed by the pre-stressing strands and confining steel. Once the pre-stressed-concrete pile has been driven to the desired depth, the dowels are grouted into the sleeves. If higher flexibility of the connection is desired, a small portion of the dowel at the top of the pile may be wrapped in Teflon to ensure de-bonding between the dowel and the grout. The dowels are then embedded in the concrete deck to provide sufficient development length. The development length of the dowel may be achieved either by outward bending of the dowel in the deck concrete or by using T-headed dowels (Roeder et al., 2005). However, the most commonly used dowel in marine oil terminals and other port facilities is the T-headed dowel as shown in Figure 1b (Restrepo et al., 2007). Note that Figure 1b shows only two outermost dowels; a typical connection may include several dowels but they are not shown here to preserve clarity in the figure.

Seismic design of marine oil terminals in California is governed by the Marine Oil Terminal Engineering and Maintenance Standard (MOTEMS) [Eskijian, 2007; MOTEMS, 2006]. The MOTEMS requires design of such facilities for two earthquake levels: Level 1 and Level 2. The return period of the design earthquake for each level depends on the risk level. For example, Level 1 and Level 2 design earthquakes for high risk terminals correspond to return periods of 72 and 475 years, respectively. The acceptance criteria for piles in the MOTEMS are specified in terms of maximum permissible material strains. The maximum permissible material strains depend on the earthquake level – Level 1 or Level 2 – and on location of the plastic hinge – pile-deck or in-ground. The material strain limits in two types of piles addressed in this paper are

summarized in Table 1.

Since the acceptance criteria in the MOTEMS is specified in terms of maximum permissible strains, evaluation of piles as per the MOTEMS provisions requires monitoring material strains during the seismic analysis. However, most commercially available structural analysis programs do not have the capability to directly monitor strains during seismic analysis. Therefore, there is a need to develop simplified acceptability criteria for piles in marine oil terminals that ensure that material strains do not exceed the values specified in the MOTEMS and yet do not require directly monitoring of strains during seismic analysis.

In order to fill this need, this investigation developed simple, closed-form formulas to estimate the displacement capacity of piles with partial-moment-connection. Development of these formulas eliminates the need to monitor material strains during the pushover analysis. Furthermore, these formulas have been shown to provide "accurate" estimate of the displacement capacity of piles.

The investigation reported in this paper presents simplified procedure for piles with partial-moment-connection. Simplified procedures for piles in which hinging is restricted to the piles is reported elsewhere (Goel, 2008a, 2008b). The investigation reported in this paper utilizes a commonly used simplifying assumption that the pile-soil-system may be represented by a simple model that is fixed at the base at a depth equal to depth-of-fixity below the mud line. The depth-to-fixity, which depends on the pile diameter and soil properties, is typically provided by the geotechnical engineer or estimated from charts available in standard textbooks on the subject (e.g., Priestley, et al., 1996) or from recommendations in several recent references (e.g., Chai, 2002; Chai and Hutchinson, 2002). Further discussion on the subject is available elsewhere (Goel 2008b) and is not included here for brevity.

BEHAVIOR OF PARTIAL-MOMENT-CONNECTION

While analyzing marine oil terminals, nonlinear behavior of pile and connection is typically represented by moment-curvature or moment-rotation relationships. These relationships are developed based on the assumption of plane section remaining plane and perfect bond between steel reinforcing bars and concrete. For the concrete-plug connection between hollow-steel piles and deck or the dowel-sleeve connection between pre-stressed-concrete pile and deck, however, such assumptions may not be valid. In particular, the pile in such connection rotates about a small area on compression side of the pile forming a gap between the top of the pile and the deck on the tension side of the pile (see Figure 2). This behavior is akin to pile acting like a crowbar bearing on the small compression area. This behavior leads to de-bonding of the dowel (or strain penetration) on each side of the joint. Additional de-bonding may also occur in the dowel over the portion that is intentionally wrapped in Teflon. Although experiments have been conducted on partial-moment-connections in piles (e.g., Restrepo et al., 2007; Roeder, et al., 2005), these experiments have not led to analytical models for partial-moment connections. Therefore, a committee of the Coasts, Oceans, Ports, and Rivers Institute (COPRI) of the American Society of Civil Engineers has recently proposed a simple analytical model for developing nonlinear moment-rotation behavior of partial-moment-connection in piles (Harn, 2008). Figure 3 shows the basic approach to develop the moment-rotation relationship of partial-moment connection; details of the procedure are included in Appendix I.

Figure 4 shows the moment rotation relationship of the concrete-plug connection for hollow steel pile and dowel-sleeve connection for pre-stressed-concrete pile. The nonlinear moment-rotation relationship (shown in solid line) has been idealized by a bilinear moment-rotation relationship (shown in dashed line). It is apparent from these results that the post-yield slope of the moment-rotation relationship is very small compared to the slope in the linear-elastic portion.

Therefore, it may be possible to simply idealize this curve with elastic-perfectly-plastic curve without much loss in accuracy.

SIMPLIFIED MODEL OF PILE WITH PARTIAL-MOMENT-CONNECTION

A pile with partial-moment-connection to the deck may be idealized as a beam-column element fixed at the base and a rotational spring at the top (Figure 5). The length of the element is equal to the free-standing height of the pile plus the depth of fixity below the mud-line. The procedure to select the depth-of-fixity is available elsewhere (see Priestley at al., 1996; Chai, 2002). The rotational spring at the top of the pile represents the nonlinear behavior of the concrete-plug or the dowel-sleeve connection. Ignoring axial deformations in the pile, this system can be modeled with two displacement degrees-of-freedom: lateral displacement, Δ, and rotation, θ, at the top. When lateral force, F, is applied at the top of the pile, a moment, M, also develops at the top of the pile because of rotational resistance provided by the rotational spring representing the concrete-plug or the dowel-sleeve connection. Note that rotation in the rotational springs is equal to rotation at top of the pile.

Presented next are the closed-form solution of the displacement capacity of this simplified model. For this purpose, let us consider an idealized moment-rotation relationship for the partial-moment-connection (Figure 6a) and idealized moment-curvature relationship of the pile section (Figure 6b). Let the initial elastic stiffness and yield moment of the partial-moment-connection be defined by k_θ and $M_{y,\mathrm{C}}$, respectively. Also let θ_L be the rotation in the rotational spring when the strain in outermost dowel of the partial-moment-connection just reaches the strain limit specified for a selected design level and θ_y be the yield rotation (Figure 6a). Let us then define the rotational ductility capacity of the connection at specified design level by

$$\mu_\theta = \frac{\theta_L}{\theta_y} \quad (1)$$

Let EI be the initial elastic slope and αEI be the post-yield slope of the idealized moment-curvature relationship; and $M_{y,P}$ be the moment and ϕ_y be the curvature at effective yielding of the pile (Figure 6b). Also let ϕ_L be the curvature of the pile section when the material strain just reaches the strain limit specified for a selected design level. Let us then define the pile section curvature ductility capacity at a selected design level as

$$\mu_\phi = \frac{\phi_L}{\phi_y} \quad (2)$$

Finally, let us define two dimensionless constants, η and β as

$$\eta = \frac{M_{y,P}}{M_{y,C}} \quad (3)$$

$$\beta = \frac{EI}{k_\theta L} \quad (4)$$

in which η is the ratio of yield moment of the pile and the connection, and β is indicative of the relative rotational stiffness of the pile and the connection.

The force-deformation behavior (or pushover curve) of a pile with fixed-base and rotational spring at the top may be idealized by a tri-linear relationship shown in Figure 6c. For piles with partial-moment-connection, the yield moment of the connection is typically selected to be smaller than yield moment of the pile section. For such condition, the first yielding in the pile-connection system would occur in the connection at lateral force and displacement equal to $F_{y,C}$ and $\Delta_{y,C}$, respectively. Since the pile has not yet reached its yield moment, the lateral force in the pile-connection system would continue to increase with displacement till yielding occurs in

the pile at force and displacement equal to $F_{y,P}$ and $\Delta_{y,P}$, respectively. Subsequently, the lateral force in the pile system would increase with displacement only due to strain-hardening effects in the pile material.

Let us define the displacement capacity of the pile with partial-moment-connection as the maximum displacement at the tip of the pile without material strains specified in the MOTEMS being exceeded either in the connection or the pile for a selected design level. It is possible that the displacement capacity may be controlled either by the material strains in the connection or in the pile. In order to demonstrate this possibility, consider the results presented in Figures 7 and 8 for the displacement ductility capacity, defined as the displacement capacity divided by the displacement at initiation of yielding in the connection, of the pile-connection system for two design levels – Level 1 and Level 2. These results were developed by nonlinear static pushover analysis of nonlinear finite element models of the pile-connection system modeled in computer program OPENSEES (McKenna and Fenves, 2001). The pile is modeled using fiber section and nonlinear beam-column elements whereas the connection is modeled with a bi-linear moment-rotation spring with moment-rotation relationship developed using the procedure described in Appendix I. During the pushover analysis, material strains in both the pile and the connection were monitored and the displacement ductility computed for two cases: material strains reaching the limiting values in the connection (designated as the connection hinge location), and material strains reaching the limiting values in the pile (designated as the pile hinge location). The results presented in Figure 7 are for hollow-steel pile of 61 cm diameter and 1.27 cm wall thickness with a concrete-plug connection having 12 dowels each with an area of 8.2 cm^2. The results in Figure 8 are for pre-stressed-concrete pile of 61 cm diameter with 16 pre-stressing strands. The area of each pre-stressing strand is equal to 1.4 cm^2, strength is 1884 MPa, and initial pre-stress in

strands is equal to 70% of its strength. The confinement is provided by #11 spiral wire (area = 0.71 cm^2) with spacing equal to 6.3 cm. The dowel connection consists of 8 bars, each with an area equal to 3.9 cm^2, and de-bonded length of 61 cm. It is useful to note that pre-stress in the strands are selected here for new pre-stressed-concrete piles. For evaluation of older piles, it is suggested that an appropriate value of pre-stress force in the strands be used.

The results presented in Figures 7 and 8 indicate that the displacement ductility for pile-hinge location tends to increase with pile length for short piles but then becomes essentially independent of the pile length for longer piles. The displacement ductility for connection hinge location, on the other hand, decreases with the pile length. As a result, pile-hinge location may control the overall displacement ductility of the pile-connection system for short piles whereas connection-hinge controls the displacement ductility of the pile-connection system for long piles. These results indicate that material strains must be monitored both in the pile (for in-ground hinging) and the connection (for deck-pile hinging) in order to establish the displacement capacity of the pile-connection system. Additional results available in Goel (2008b) also support this conclusion.

DISPLACEMENT CAPACITY OF PILE WITH PARTIAL-MOMENT-CONNECTION

The displacement capacity of the pile with partial moment capacity is given by

$$\Delta = \mu_\Delta \Delta_{y,C} \tag{5}$$

in which

$$\Delta_{y,C} = \frac{\theta_{y,C} L (1+4\beta)}{6\beta} \tag{6}$$

is the yield displacement which corresponds to first effective yielding in the connection (see Figure 6c), and μ_Δ is the displacement ductility capacity of the pile defined as lower of the

displacement ductility capacity corresponding to yielding in the connection, $\mu_{\Delta,C}$ and the displacement ductility capacity corresponding to yielding in the pile, $\mu_{\Delta,P}$. The ductility $\mu_{\Delta,C}$ is given by

$$\mu_{\Delta,C} = \begin{cases} \dfrac{1+4\beta\mu_\theta}{1+4\beta} & \text{for } \mu_\theta \le \dfrac{\eta-1}{2\beta} \\ \dfrac{2-\eta+6\beta\mu_\theta}{1+4\beta} & \text{for } \mu_\theta > \dfrac{\eta-1}{2\beta} \end{cases} \tag{7}$$

Equation (7) provides the value of $\mu_{\Delta,C}$ for two cases: strain limits in the connection reaching the specified values prior to or after initiation of yielding in the pile. The ductility $\mu_{\Delta,P}$ is given by

$$\mu_{\Delta,P} = \frac{2\eta-1}{1+4\beta} + \left(\frac{6\eta}{1+4\beta}\right)\left(\frac{\rho\eta}{1+\eta}\right)\left(1-\frac{\rho\eta}{2(1+\eta)}\right)(\mu_\phi - 1) \tag{8}$$

in which ρ is the length of the plastic hinge in the pile as a fraction of its length. The recommended value is $\rho = 0.03$ for Level 1 design and $\rho = 0.075$ for Level 2 design of hollow-steel piles with concrete-plug connection; and $\rho = 0.05$ for both design levels of pre-stressed-concrete pile with dowel-sleeve connection. These values are based on calibration of results against those from finite element analysis. It may be appropriate to further verify these values from experimental observations. A detailed derivation of the results of Equations (6) to (8) is presented in Appendix II.

Step-by-Step Summary

Following is a step-by-steel summary of the procedure to compute displacement capacity of piles with partial-moment-connection:

1. Establish the axial load, P, on the pile.
2. Estimate the pile length based on equivalent depth-of-fixity assumption.

3. Select an appropriate design level – Level 1 or Level 2 – and establish various strain limits for the selected design level.
4. Develop the moment-rotation relationship of the partial-moment-connection using the procedure described in Appendix I. This relationship could also be developed from any other rational procedure.
5. Determine rotational stiffness, k_{θ}, yield moment, $M_{y,C}$, and yield rotation, $\theta_{y,C}$ of the connection from the moment-rotation relationship developed in Step 4.
6. Establish the rotation of the connection, θ_L, and corresponding connection rotational ductility capacity, $\mu_{\theta} = \theta_L / \theta_{y,C}$, when strain in the outer-most dowel of the connection reaches the strain limit established in Step 3 for the selected design level.
7. Conduct the moment-curvature analysis of the pile section and idealize the moment-curvature relationship by a bi-linear curve. For this analysis, apply the axial load on the pile prior to moment-curvature analysis.
8. Compute the effective, EI_e, and effective yield moment, $M_{y,P}$, from the pile moment-curvature relationship. Note that EI_e is equal to initial elastic slope and $M_{y,P}$ is the yield value of the moment of the idealized bi-linear moment-curvature relationship. For steel piles, EI may be computed from section properties and material modulus, and $M_{y,P}$ may be approximated as $M_{y,P} = f_y \left(d_o^3 - d_i^3 \right) / 6$, thus eliminating the need for Step 7.
9. Estimate the yield curvature, $\phi_{y,P} = M_{y,P} / EI_e$.
10. Establish the curvature of the pile, ϕ_L, and corresponding section curvature ductility capacity, $\mu_{\phi} = \phi_L / \phi_{y,P}$, when material strain in the pile section reaches the strain limit established in Step 3 for the selected design level.
11. Select the value of ρ which defines the length of the plastic hinge as a fraction of the pile length.
12. Compute the dimensionless parameters: $\eta = M_{y,P} / M_{y,C}$, and $\beta = EI_e / k_{\theta} L$.

13. Compute the yield displacement which corresponds to first effective yielding in the connection as: $\Delta_{y,C} = \theta_{y,C} L(1+4\beta)/6\beta$

14. Compute the displacement ductility for yielding in the connection as $\mu_{\Delta,C} = (1+4\beta\mu_\theta)/(1+4\beta)$ if μ_θ computed in Step 6 is less than or equal to $(\eta-1)/2\beta$ otherwise $\mu_{\Delta,C} = (2-\eta+6\beta\mu_\theta)/(1+4\beta)$.

15. Compute displacement ductility for yielding in the pile as $\mu_{\Delta,P} = (2\eta-1)/(1+4\beta)+(6\eta)(\rho\eta/1+\eta)(1-\rho\eta/2+2\eta)(\mu_\phi-1)/(1+4\beta)$

16. Establish the displacement ductility capacity as lower of the values computed in Steps 14 and 15.

17. Compute the displacement capacity of the pile as product of the yield displacement computed in Step13 and the displacement ductility capacity computed in Step 16.

ANALTYICAL EVALUATION OF CLOSED-FORM FORMULAS

The accuracy of the closed-form formulas developed in Appendix II and summarized in the preceding section is evaluated next by comparing design ductility capacity from nonlinear finite element analysis (NFEA) with that from Equations (7) and (8). Figures 9 and 10 present the results for a 61 cm diameter hollow-steel pile for seismic design level 1 and 2, respectively. The results are for two wall thicknesses, 1.27 cm and 2.54 cm; two values of pile axial load, $0.05Af_y$ and $0.1Af_y$; and two arrangement of dowels, 8 or 12, in the connection. The area of each dowel is 8.2 cm^2. The combination of these parameters is indicated on each figure. Similarly, Figures 11 and 12 present the results for pre-stressed-concrete pile for design levels 1 and 2, respectively. The selected pile is of 61 cm diameter with 16 pre-stressing strands. The area of each pre-stressing strand is equal to 1.4 cm^2, strength is 1884 MPa, and initial pre-stress in strands is equal to 70% of its strength. The confinement is provided by #11 spiral wire (area = 0.71 cm^2) with spacing equal to 6.3 cm. The dowel connection consists of 8 bars, each with an area equal to 3.9

cm^2. Four different values of de-bonded lengths – 0, 30, 61, and 91 cm – are selected. The results from nonlinear finite element were generated, as noted previously, using OPENSEES (McKenna and Fenves). The details of material models and modeling assumptions are available in Goel (2008b).

The presented results in Figures 9 to 12 indicate that the closed-form formulas developed in this investigation provide "accurate" estimate of displacement ductility capacity of hollow-steel piles with concrete-plug connection (Figures 9 and 10) as well as for pre-stressed-concrete piles with dowel-sleeve connection (Figures 11 and 12). This becomes apparent from essentially identical curves for the displacement ductility obtained from the closed-form formulas and the nonlinear finite element analysis. For very-short pre-stressed-concrete piles, the closed-form formulas provide values of the displacement ductility capacity that is lower than the values from the nonlinear finite element analysis for the MOTEMS seismic design Level 2 (Figure 12). However, the estimate of the displacement ductility from the closed-form formulas is a lower-bound, and hence conservative, estimate. Additional results presented in Goel (2008b) also confirm this observation.

The results presented so far indicate that the simplified pile-connection system utilized to develop the closed-form formulas for the displacement ductility capacity of the piles with partial-moment-connection provides very "good" estimate of the displacement ductility capacity. These formulas utilize the curvature ductility capacity of the pile section and rotation ductility capacity of the connection, along with the parameter β which depends on the relative stiffness of the pile and the connection and the parameter η which depends on the relative strength of the connection and the pile. This information is readily available from the pile section moment-curvature analysis and connection moment-rotation analysis. The implementation of the closed-form

formulas can be further simplified by developing design charts for commonly used piles section details and connection details thus eliminating the need for pile section moment-curvature analysis and the connection moment-rotation analysis.

CONCLUSION

In this investigation, a simplified model of the pile with partial-moment-connection has been utilized to develop closed-form formulas for estimating the displacement capacity of piles typically used in the marine oil terminals. The displacement capacity estimated from these formulas ensures that the material stain limits specified in the MOTEMS is not exceeded. These formulas are demonstrated to be "accurate" by comparing results from these formulas against those from the nonlinear finite-element analysis.

The formulas developed in this investigation utilize the curvature ductility capacity of the pile section and rotation ductility capacity of the connection at the selected seismic design level in the MOTEMS, along with the parameter β which depends on the relative stiffness of the pile and the connection and the parameter η which depends on the relative strength of the connection and the pile. This information is readily available from the pile section moment-curvature analysis and connection moment-rotation analysis. The implementation of the closed-form formulas can be further simplified by developing design charts for commonly used piles section details and connection details thus eliminating the need for pile section moment-curvature analysis and the connection moment-rotation analysis.

It must be noted that the procedure developed in this investigation has been verified against results from nonlinear finite element analysis. It would be useful to verify this procedure against experimental results as well.

ACKNOWLDEGMENT

This research investigation is supported by the California State Lands Commission (CSLC) under Contract No. C2005-051 with Martin Eskijian as the project manager. This support is gratefully acknowledged.

APPENDIX I: MOMENT-ROTATION RELATIONSHIP OF PARTIAL-MOMENT CONNECTION

Practicing engineers have recently proposed a simple analytical model (Figure 3) for developing nonlinear moment-rotation behavior of partial-moment-connection in piles (Harn, 2008). For a selected value of the reinforcing bar yield stress, f_y, concrete strength, $f_c^{'}$, diameter and area of reinforcing bars, d_{bi} and A_{si}, respectively, bearing strength of deck concrete against pile concrete as $f_m^{'} = 1.7 f_c^{'}$, and bearing strength of deck concrete against steel shell of hollow steel pile as $f_m^{'} = 5.6 f_c^{'}$, the moment rotation relationship is developed as follows:

1. Select a value of strain in the outermost dowel on the tension side, ε_1. Typically the first strain value is selected as the yield strain in steel, ε_y.
2. Establish the location of the neutral axis of the section by the following iterative procedure:
   2.1. Guess the location of the neutral axis.
   2.2. Calculate strains in all dowels.
   2.3. Calculate forces in all dowels, T_i. Note that dowel forces would be tensile on the tension side of the neutral axis and compressive on the compression side of the neutral axis.
   2.4. Calculate compressive force, C_c, in concrete on compression side of the neutral axis.
   2.5. Calculate compressive force, C_s, due to bearing of steel shell against the deck for hollow steel piles. Note that this step would not be necessary for prestressed concrete piles.

2.6. Calculate the summation of all forces, including any axial force on the pile. Repeat Steps 2.1 to 2.5 till this summation of forces is essentially equal to zero.

3. Estimate the length of strain-penetration in the dowel: $L_{sp} = 0.15 f_s d_b + L_{db}$ in which f_s is the dowel stress in units of ksi, d_b is the dowel diameter in inch, and L_{db} is the length of de-bonded reinforcing bar (as may be the case for prestressed concrete piles). Alternatively, the strain penetration length may be selected as $L_{sp} = 5d_b + L_{db}$ or as per the recommendations by Raynor et al. (2002).
4. Compute the elongation of the outermost dowel: $\Delta L_1 = \varepsilon_1 L_{sp}$.
5. Compute the rotation of the concrete-plug connection: $\theta = \Delta L_1 / Y_1$ in which Y_1 is the distance between neutral axis and the outermost dowel on the tension side of the neutral axis.
6. Compute the moment, M , as summation of moments at center of the pile due to tensile as well compressive forces.
7. Repeat Steps 1 to 6 to develop the entire moment-rotation relationship of the connection.
8. Idealize the moment-rotation relationship by a bi-linear curve.

APPENDIX II: DERIVATION OF DISPLACEMENT CAPACITY OF PILE WITH PARTIAL-MOMENT-CONNECTION

This appendix presents the derivation of the closed-form formulas for estimating the displacement ductility capacity of piles with partial-moment-connection. For this purpose, a simplified pile-connection system (Figure 5) and the idealized nonlinear behavior of the pile-section, connection, and the pile-connection system (Figure 6) have been utilized. Following is the detailed derivation of these formulas:

Response at First Yielding in Connection

To compute the rotation and deflection at top of the hollow steel pile with concrete-plug in the initial elastic region, i.e., $\Delta \le \Delta_{y,C}$, consider the cantilever with a moment equal to $k_\theta \theta$ and lateral force equal to F at the top (Figure 13a) with bending moment diagram (Figure 13b) and the curvature diagram (Figure 13c). Using moment-area method for structural analysis, the

rotation and deflection at the top of the pile are given by

$$\theta = \frac{FL^2}{2EI} - \frac{k_\theta L\theta}{EI} = \frac{FL^2}{2EI} - \frac{\theta}{\beta} \tag{9}$$

and

$$\Delta = \frac{FL^3}{3EI} - \frac{k_\theta \theta L^2}{2EI} = \frac{FL^3}{3EI} - \frac{\theta L}{2\beta} \tag{10}$$

Equation (9) can be further simplified to obtain the rotation as

$$\theta = \left(\frac{FL^2}{2EI}\right)\left(\frac{\beta}{1+\beta}\right) \tag{11}$$

Utilizing Equation (11), Equation (10) can also be simplified to obtain the deflection as

$$\Delta = \left(\frac{FL^3}{12EI}\right)\left(\frac{1+4\beta}{1+\beta}\right) \tag{12}$$

The first yielding in the pushover curve (Figure 6) occurs at yielding of the connection at yield rotation at the top of the pile equal to

$$\theta_{y,C} = \frac{M_{y,C}}{k_\theta} \tag{13}$$

Utilizing Equation (13) in Equation (11) gives the lateral force at the yield level as

$$F_{y,C} = \frac{2M_{y,C}}{L}(1+\beta) \tag{14}$$

and utilizing Equation (14) in Equation (12) gives the yield displacement as

$$\Delta_{y,C} = \frac{M_{y,C}L^2}{6EI}(1+4\beta) = \frac{k_\theta \theta_{y,C} L^2}{6EI}(1+4\beta) = \theta_{y,C} L\left(\frac{1+4\beta}{6\beta}\right) \tag{15}$$

Response at First Yielding in Pile

The response in the range $\Delta_{y,C} \le \Delta \le \Delta_{y,P}$ may be computed by an incremental approach in

which the system may be treated as a cantilever fixed at the base and free at the top (Figure 14). For this system, the incremental displacement and rotation at the top are given by

$$\left(\Delta-\Delta_{y,C}\right)=\frac{L^3}{3EI}\left(F-F_{y,C}\right) \tag{16}$$

$$\left(\theta-\theta_{y,C}\right)=\frac{L^2}{2EI}\left(F-F_{y,C}\right) \tag{17}$$

which lead to the expression for the total displacement and rotation as

$$\Delta=\Delta_{y,C}+\frac{L^3}{3EI}\left(F-F_{y,C}\right)=\frac{M_{y,C}L^2}{6EI}\left(1+4\beta\right)+\frac{L^3}{3EI}\left(F-F_{y,C}\right) \tag{18}$$

$$\theta=\theta_{y,\mathrm{C}}+\frac{L^2}{2EI}\left(F-F_{y,\mathrm{C}}\right)=\frac{M_{y,\mathrm{C}}}{k_\theta}+\frac{L^2}{2EI}\left(F-F_{y,\mathrm{C}}\right) \tag{19}$$

The lateral force at when the pile yields can be computed from equilibrium of the cantilever (Figure 14d) as

$$F_{y,P}=\frac{M_{y,C}+M_{y,P}}{L} \tag{20}$$

Utilizing Equation (20) in Equations (18) and (19) leads to displacement and rotation at yielding of the pile as

$$\begin{aligned}\Delta_{y,P}&=\frac{M_{y,C}L^2}{6EI}\left(1+4\beta\right)+\frac{L^3}{3EI}\left(F_{y,P}-F_{y,C}\right)\\&=\frac{M_{y,C}L^2}{6EI}\left(1+4\beta\right)+\frac{M_{y,P}L^2}{3EI}+\frac{M_{y,C}L^2}{3EI}-\frac{2M_{y,C}}{L}\left(1+\beta\right)\frac{L^3}{3EI}\\&=\left(\frac{M_{y,P}L^2}{3EI}\right)\left(\frac{2\eta-1}{2\eta}\right)\end{aligned} \tag{21}$$

$$
\begin{aligned}
\theta_{y,P} &= \frac{M_{y,C}}{k_\theta} + \frac{L^2}{2EI}\left(F_{y,P} - F_{y,C}\right) \\
&= \frac{M_{y,C}}{k_\theta} + \frac{M_{y,P}L}{2EI} + \frac{M_{y,C}L}{2EI} - \frac{2M_{y,C}}{L}\left(1+\beta\right)\frac{L^2}{2EI} \\
&= \left(\frac{M_{y,P}L}{2EI}\right)\left(\frac{\eta-1}{\eta}\right)
\end{aligned}
\tag{22}
$$

Displacement Ductility Capacity of Pile

Developed next are the formulas for computing displacement ductility capacity of piles with partial-moment connection. These formulas are developed in two stages: the ductility controlled by material strain limits in the connection; and ductility controlled by material strains in the pile section. The displacement ductility capacity is then defined as the lower of the two ductility values.

Strain Limits in the Connection

Let θ_L be the rotation in the connection spring for a selected design level, i.e., specified value of strain in outermost dowel for a selected design level. For the pile-connection system, this rotation may occur either prior to pile yielding, i.e., $\theta_{y,C} < \theta_L < \theta_{y,P}$, or after pile yielding, i.e., $\theta_L > \theta_{y,P}$. The connection rotation ductility at onset of pile yielding is given by

$$
\begin{aligned}
\mu_{\theta,P} &= \frac{\theta_{y,P}}{\theta_{y,C}} = \frac{k_\theta}{M_{y,C}}\left(\frac{M_{y,P}L}{2EI}\right)\left(\frac{\eta-1}{\eta}\right) \\
&= \left(\frac{M_{y,P}}{M_{y,C}}\right)\left(\frac{k_\theta L}{2EI}\right)\left(\frac{\eta-1}{\eta}\right) \\
&= \frac{\eta-1}{2\beta}
\end{aligned}
\tag{23}
$$

The displacement capacity of the pile-connection system by considering strain limits in outermost dowel of the connection depends on whether the pile remains elastic or pile yields when the dowel strain limit is reached. Note that the pile would remain elastic if μ_θ is less than

$\mu_{\theta,P}$ given by Equation (23). If the pile remains elastic, the rotation in the plug at selected design level, θ_L, is related to the lateral force F by Equation (19) as

$$\theta_L = \theta_{y,C} + \frac{L^2}{2EI}\left(F - F_{y,C}\right) \tag{24}$$

which gives

$$\left(F - F_{y,C}\right) = \left(\theta_L - \theta_{y,C}\right)\left(\frac{2EI}{L^2}\right) = \theta_{y,C}\left(\mu_\theta - 1\right)\left(\frac{2EI}{L^2}\right) \tag{25}$$

Using Equation (18), the displacement is then given as

$$\begin{aligned}\Delta_L &= \frac{M_{y,C}L^2}{6EI}(1+4\beta) + \frac{L^3}{3EI}\theta_{y,C}\left(\mu_\theta - 1\right)\left(\frac{2EI}{L^2}\right) \\ &= \frac{\theta_{y,C}k_\theta L^2}{6EI}(1+4\beta) + \frac{2L}{3}\theta_{y,C}\left(\mu_\theta - 1\right) \\ &= \theta_{y,C}L\left[\frac{1+4\beta}{6\beta} + \frac{2\left(\mu_\theta - 1\right)}{3}\right]\end{aligned} \tag{26}$$

The displacement ductility capacity is then defined as

$$\begin{aligned}\mu_\Delta &= \frac{\Delta_L}{\Delta_{y,C}} = \frac{\theta_{y,C}L\left[\frac{1+4\beta}{6\beta} + \frac{2\left(\mu_\theta - 1\right)}{3}\right]}{\theta_{y,C}L\left(\frac{1+4\beta}{6\beta}\right)} = 1 + \left(\mu_\theta - 1\right)\left(\frac{4\beta}{1+4\beta}\right) \\ &= \frac{1+4\beta\mu_\theta}{1+4\beta}\end{aligned} \tag{27}$$

If the pile yields prior to the connection reaching θ_L, i.e., if μ_θ is more than $\mu_{\theta,P}$, the deflection at the pile top can be approximated as

$$\Delta_L = \Delta_{y,P} + \left(\theta_L - \theta_{y,P}\right)L \tag{28}$$

which can be re-written as

$$
\begin{aligned}
\Delta_L &= \Delta_{y,P} + \theta_{y,C} L \left(\mu_\theta - \frac{\theta_{y,P}}{\theta_{y,C}} \right) \\
&= \Delta_{y,C} + \frac{M_{y,P} L^2}{3EI} + \frac{M_{y,C} L^2}{3EI} - \frac{2M_{y,C}}{L}(1+\beta)\frac{L^3}{3EI} + \theta_{y,C} L \left(\mu_\theta - \frac{\eta - 1}{2\beta} \right)
\end{aligned}
\tag{29}
$$

The displacement ductility capacity is then defined as

$$
\begin{aligned}
\mu_\Delta &= \frac{\Delta_L}{\Delta_{y,C}} = 1 + \frac{1}{\dfrac{M_{y,C} L^2}{6EI}(1+4\beta)} \left[\begin{array}{l} \dfrac{M_{y,P} L^2}{3EI} + \dfrac{M_{y,C} L^2}{3EI} - \dfrac{2M_{y,C}}{L}(1+\beta)\dfrac{L^3}{3EI} \\ +\theta_{y,C} L \left(\mu_\theta - \dfrac{\eta - 1}{2\beta} \right) \end{array} \right] \\
&= \frac{2 - \eta + 6\beta\mu_\theta}{1+4\beta}
\end{aligned}
\tag{30}
$$

The displacement ductility capacity of the pile-concrete-plug system can be summarized as

$$
\mu_\Delta = \begin{cases} \dfrac{1+4\beta\mu_\theta}{1+4\beta} & \text{for } \mu_\theta \le \dfrac{\eta-1}{2\beta} \\ \dfrac{2-\eta+6\beta\mu_\theta}{1+4\beta} & \text{for } \mu_\theta > \dfrac{\eta-1}{2\beta} \end{cases}
\tag{31}
$$

Equation (31) applies only for displacement ductility capacity when the strain in outermost fiber of the dowel in the connection reaches the strain limit for a selected design level.

Strain Limits in the Pile

The preceding section developed the expression for displacement ductility capacity of the pile-connection system controlled by the strain limit in dowel of the connection. However, it is possible that the strain limit in the pile may occur prior to the system reaching the displacement-ductility capacity given by Equation (31). Therefore, relationship for displacement-ductility of the pile-connection system at strain limits in the pile is developed next.

Let us consider the equilibrium of the pile when the strain limit reaches the limiting value at a selected design level (Figure 15). The moment at the top of the pile is equal to $M_{y,C}$ and at the

bottom is equal to $M_{y,P}$. The length L_2 is then given by

$$L_2 = \frac{\eta}{1+\eta} L \tag{32}$$

Let up define the plastic hinge length as

$$L_p = \rho L_2 \tag{33}$$

in which ρ is length of the plastic hinge as a fraction of the "effective" length defined as the distance from the critical section to the point of contra-flexure ($= L_2$ for this case). Using Equation (32) in Equation (33) gives plastic hinge length normalized by the total pile length as

$$L_p^* = \frac{L_p}{L} = \frac{\rho\eta}{1+\eta} \tag{34}$$

Using concepts similar to those developed for piles with perfect moment connection (Goel, 2008a, 2008b), the displacement capacity of the pile is given by

$$\begin{aligned}
\Delta_L &= \Delta_{y,P} + \left(L - \frac{L_p}{2}\right)\left[L_p\left(\phi_L - \phi_y\right)\right] \\
&= \Delta_{y,P} + \phi_y L^2 \left(1 - \frac{L_p^*}{2}\right)\left(L_p^*\right)\left(\mu_\phi - 1\right) \\
&= \Delta_{y,P} + \left(\frac{M_{y,\mathrm{P}} L^2}{EI}\right)\left(1 - \frac{L_p^*}{2}\right)\left(L_p^*\right)\left(\mu_\phi - 1\right)
\end{aligned} \tag{35}$$

Dividing Equation (35) by the yield displacement given by Equation (15), the displacement-ductility capacity is given by

$$\begin{aligned}
\mu_\Delta = \frac{\Delta_L}{\Delta_{y,C}} &= \frac{2\eta - 1}{1+4\beta} + \left(\frac{6\eta L_p^*}{1+4\beta}\right)\left(1 - \frac{L_p^*}{2}\right)\left(\mu_\phi - 1\right) \\
&= \frac{2\eta - 1}{1+4\beta} + \left(\frac{6\eta}{1+4\beta}\right)\left(\frac{\rho\eta}{1+\eta}\right)\left(1 - \frac{\rho\eta}{2\left(1+\eta\right)}\right)\left(\mu_\phi - 1\right)
\end{aligned} \tag{36}$$

Equation (36) applies only for displacement ductility capacity when the material strain in the pile

reaches the strain limit for a selected design level, i.e., hinging in the pile.

REFERENCES

Chai, Y.H. (2002). "Flexural strength and ductility of extended pile-shafts. I: Analytical model," *Journal of Structural Engineering*, 128(5):586-594.

Chai, Y.H. and Hutchinson, T.C. (2002). "Flexural strength and ductility of extended pile-shafts. II: Experimental study," *Journal of Structural Engineering*, 128(5):595-602.

Eskijian, M. (2007). "Marine Oil Terminal Engineering and Maintenance Standards (MOTEMS)," *Proceedings of 2007 Structures Congress*, ASCE, Long Beach, CA.

Ferritto, J., Deckenson, S., Priestley, N., Werner, S. and Taylor, C. (1999). Seismic criteria for California marine oil terminals, *Technical Report No. TR-2103-SHR*, Naval Facilities Engineering Service Center, Shore Facilities Department, Structures Division, Port Hueneme, CA.

Goel, R.K. (2008a). "Simplified procedure for seismic analysis of piles in marine oil terminals," *Proceedings of 2008 Structures Congress*, ASCE, Vancouver, B.C., Canada.

Goel R.K. (2008b). "Simplified procedures for seismic analysis and design of piers and wharves in marine oil and LNG terminals," Draft *Report No. CP/SEAM-08/01*, California Polytechnic State University, San Luis Obispo, CA

Harn, R. (2008). "Moment-rotation behavior of pile to cap connection," Personal communication, Berger/ABAM Engineers Inc.

Klusmeyer, L. and Harn, R. (2004). "Displacement-based seismic design of large naval pier." *Proceedings of PORTS 2004*, Houston, TX, May 23-26.

McKenna, F. and Fenves, G. (2001). *The OpenSees Command Language Manual: version 1.2*, Pacific Earthquake Engineering Center, University of California, Berkeley. <http://opensees.berkeley.edu>

MOTEMS (2006). *Marine Oil Terminal Engineering and Maintenance Standards*, Chapter 31F (Marine Oil Terminals), Title 24, California Code of Regulations, Part 2, California Building Code, Published by the California State Lands Commission, Long Beach, CA. <http://www.slc.ca.gov/Division_pages/MFD/MOTEMS.html>

Nezamian, A., Al-Mahaidi, R., and Grundy, P. (2006). “Bond strength of concrete plugs embedded in tubular steel piles under cyclic loading.” *Canadian Journal of Civil Engineering*, 33(2):111-125.

Park, R.J.T., Priestly, M.J.N., and Berrill, J.B. (1987). Seismic performance of steel-encased concrete piles. *Report No. 87-5*, Department of Civil Engineering, University of Canterbury, N.Z.

Priestley, M.J.N. and Park, R. (1984). Strength and ductility of bridge substructures. *Report No. 84-20*, Department of Civil Engineering, University of Canterbury, N.Z.

Priestley, M.J.N, Seible, F. and Calvi, G.M. (1996). *Seismic Design and Retrofit of Bridges*. John Wiley and Sons, Inc. New York.

Raynor, D.J., Lehman, D.E., and Stanton, J.F. (2002). “Bond-slip response of reinforcing bars grouted in ducts.” *Structural Journal*, ACI, 99(5):568-576.

Restrepo, J.I, Yin, P., Jaradat, O., and Weismair, M. (2007). “Performance of new pile-deck connections under earthquakes,” *Proceedings of 2007 Structures Congress*, ASCE, Long Beach, CA.

Roeder, C.W., Graff, R., Sonderstrom, J., and Yoo, J.H. (2005). “Seismic performance of pile-wharf connections.” *Journal of Structural Engineering*, 131(3):428-437.

Wray, M., Harn, R., and Jacob, J. (2007). “Port of Everett rail/barge transfer facility seismic design Everett, Washington.” *Proceedings of PORTS 2007*, San Diego, CA, March 25-28.

LIST OF TABLES

LIST OF FIGURES

Figure 15. Equilibrium of the pile when strain reaches limiting value in the pile-hinge.

Figure 1

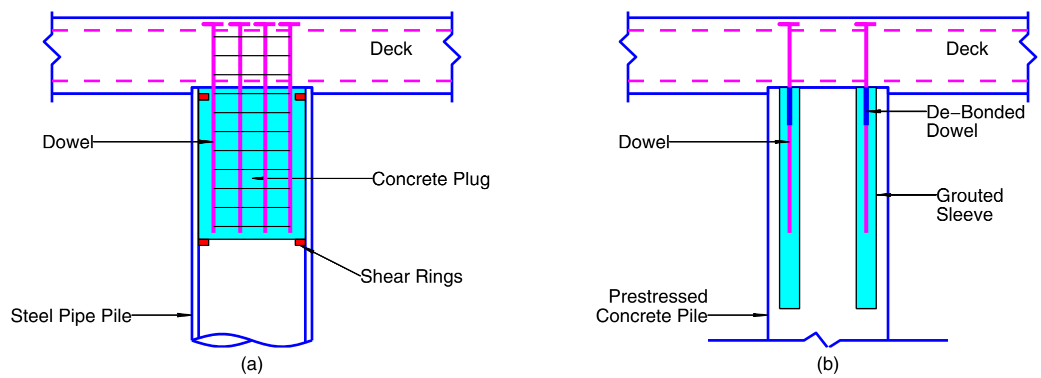

Deck
Dowel
Concrete Plug
Shear Rings
Steel Pipe Pile
(a)
Deck
De–Bonded
Dowel
Dowel
Grouted
Sleeve
Prestressed
Concrete Pile
(b)

Figure 2

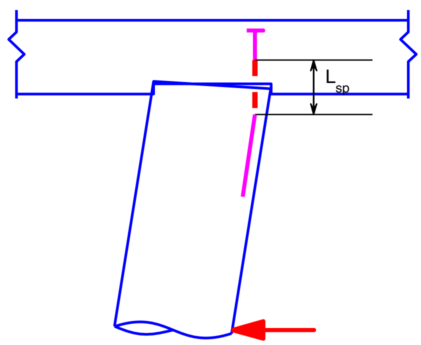

Figure 3

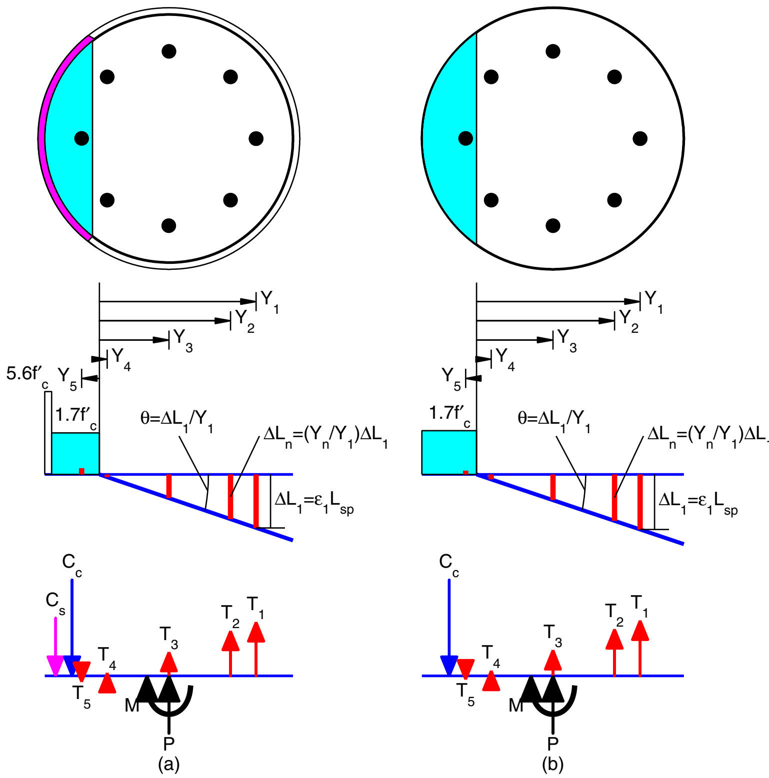

Y1
Y2
Y3
Y4
Y5
5.6f′c
1.7f′c
θ=ΔL1/Y1
ΔLn=(Yn/Y1)ΔL1
ΔL1=ε1Lsp
Cc
Cs
T1
T2
T3
T4
T5
M
P
(a)
(b)

Figure 4

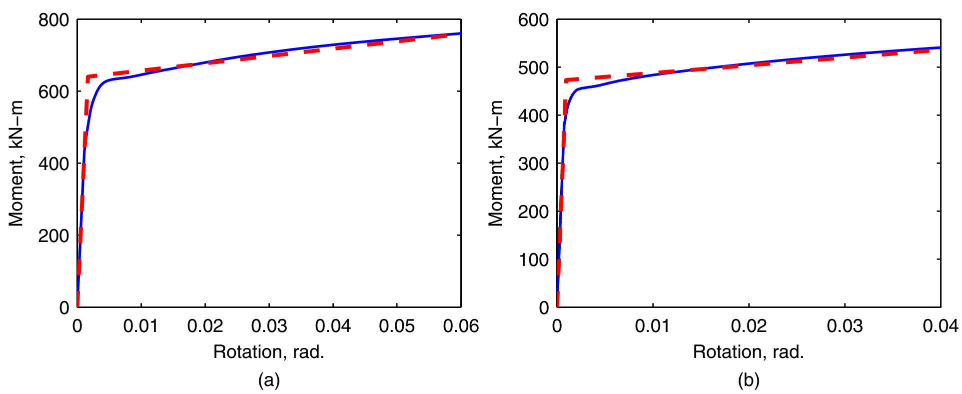
Moment, kN−m
800
600
400
200
0
0
0.01
0.02
0.03
0.04
0.05
0.06
Rotation, rad.
(a)
Moment, kN−m
600
500
400
300
200
100
0
0
0.01
0.02
0.03
0.04
Rotation, rad.
(b)

Figure 5

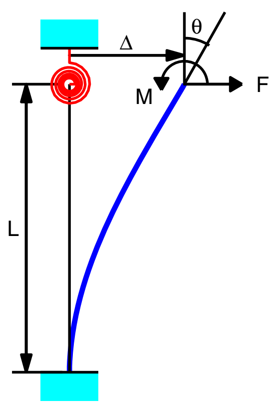

Figure 6

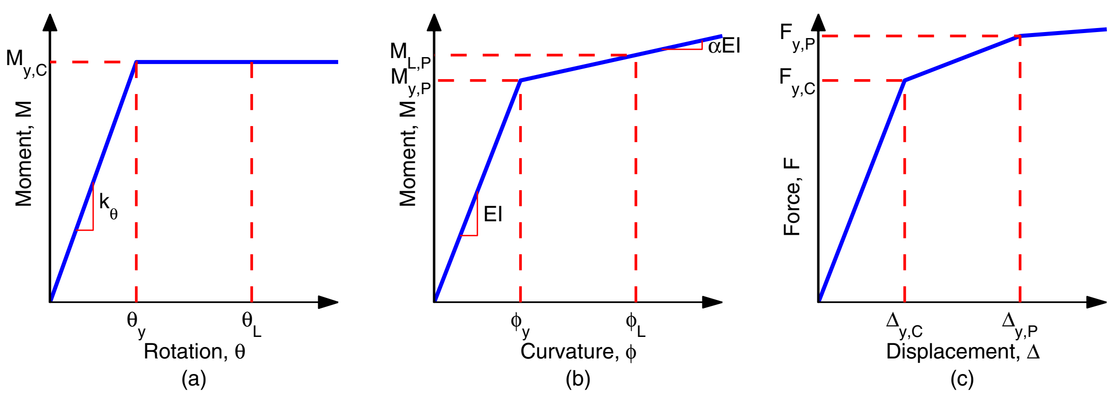

M y,C
Moment, M
k θ
θ y
θ L
Rotation, θ
(a)
M L,P
M y,P
Moment, M
EI
αEI
ϕ y
ϕ L
Curvature, ϕ
(b)
F y,P
F y,C
Force, F
Δ y,C
Δ y,P
Displacement, Δ
(c)

Figure 7

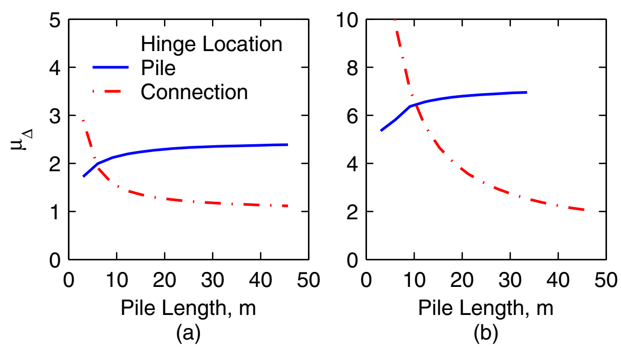

Hinge Location
Pile
Connection
μ_Δ
Pile Length, m
(a)
Pile Length, m
(b)

Figure 8

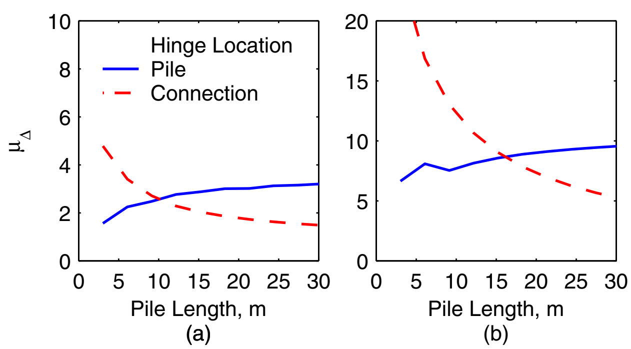

10
8
6
4
2
0
μ_Δ
Hinge Location
Pile
Connection
0 5 10 15 20 25 30
Pile Length, m
(a)
20
15
10
5
0
0 5 10 15 20 25 30
Pile Length, m
(b)

Figure 9

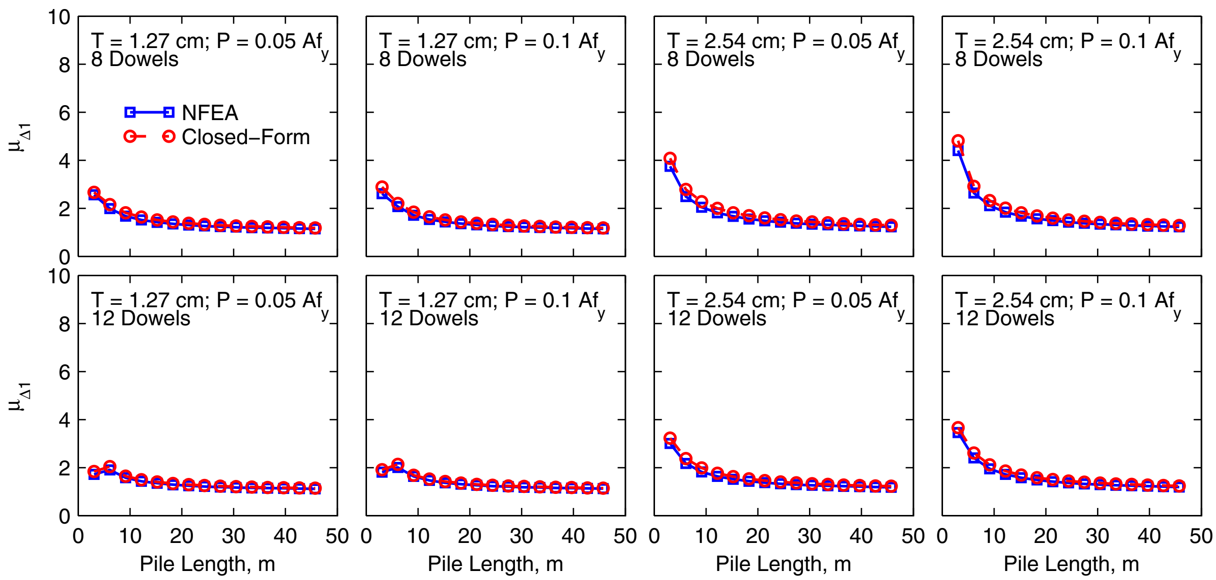

T = 1.27 cm; P = 0.05 Af
y
8 Dowels
NFEA
Closed−Form
T = 1.27 cm; P = 0.1 Af
y
8 Dowels
T = 2.54 cm; P = 0.05 Af
y
8 Dowels
T = 2.54 cm; P = 0.1 Af
y
8 Dowels
T = 1.27 cm; P = 0.05 Af
y
12 Dowels
T = 1.27 cm; P = 0.1 Af
y
12 Dowels
T = 2.54 cm; P = 0.05 Af
y
12 Dowels
T = 2.54 cm; P = 0.1 Af
y
12 Dowels
μ
Δ1
Pile Length, m
0
2
4
6
8
10
0
10
20
30
40
50

Figure 10

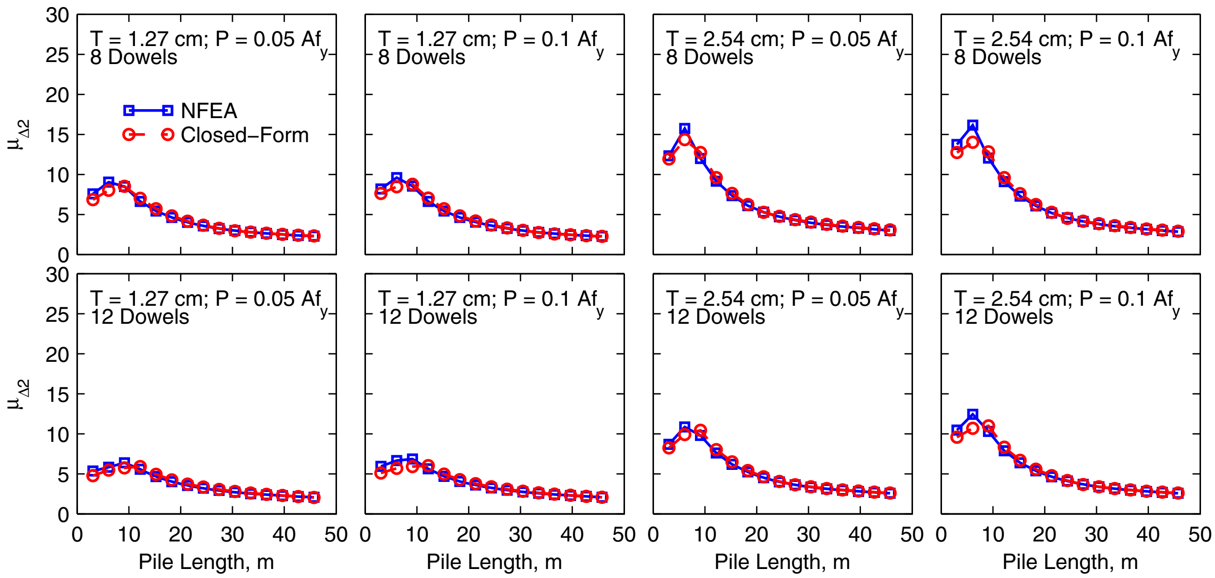

T = 1.27 cm; P = 0.05 Af_y
8 Dowels
NFEA
Closed−Form
T = 1.27 cm; P = 0.1 Af_y
8 Dowels
T = 2.54 cm; P = 0.05 Af_y
8 Dowels
T = 2.54 cm; P = 0.1 Af_y
8 Dowels
T = 1.27 cm; P = 0.05 Af_y
12 Dowels
T = 1.27 cm; P = 0.1 Af_y
12 Dowels
T = 2.54 cm; P = 0.05 Af_y
12 Dowels
T = 2.54 cm; P = 0.1 Af_y
12 Dowels
μ_Δ2
Pile Length, m

Figure 11

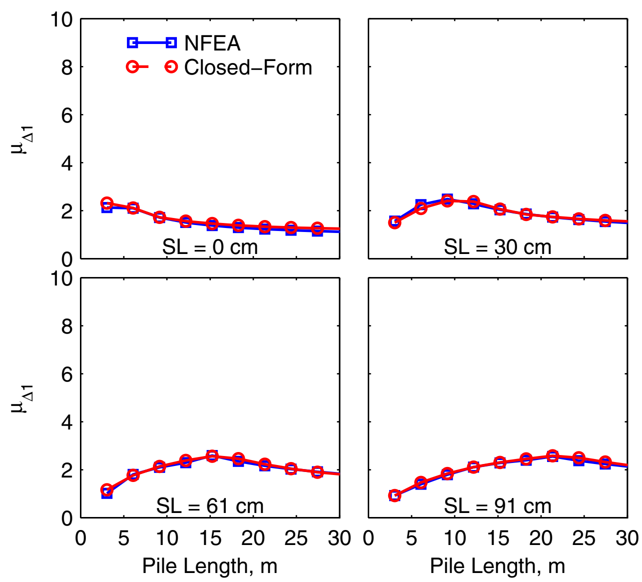

NFEA
Closed−Form
$\mu_{\Delta 1}$
SL = 0 cm
SL = 30 cm
SL = 61 cm
SL = 91 cm
Pile Length, m
Pile Length, m

Figure 12

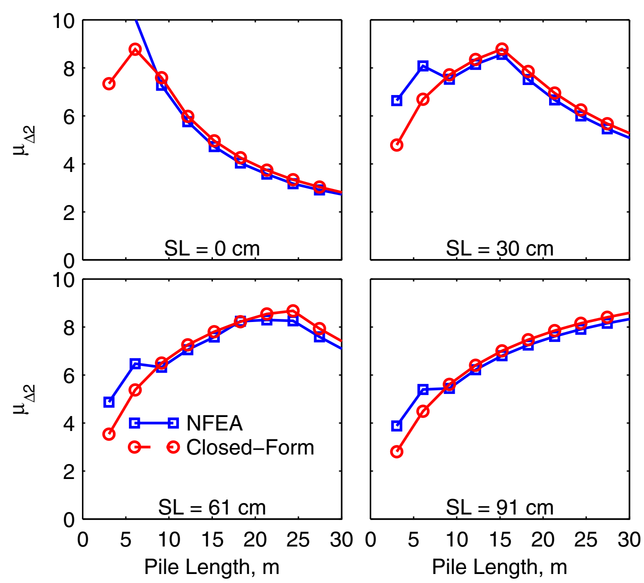

$\mu_{\Delta 2}$
SL = 0 cm
SL = 30 cm
SL = 61 cm
SL = 91 cm
NFEA
Closed−Form
Pile Length, m

Figure 13

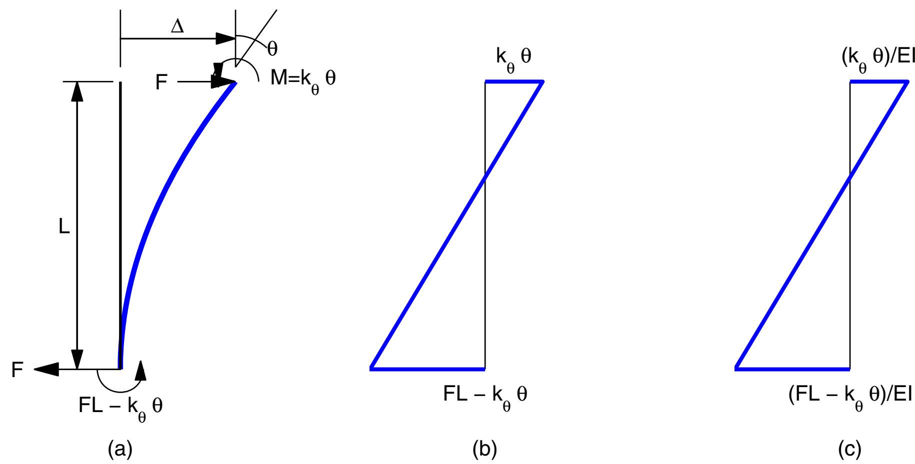

Figure 14

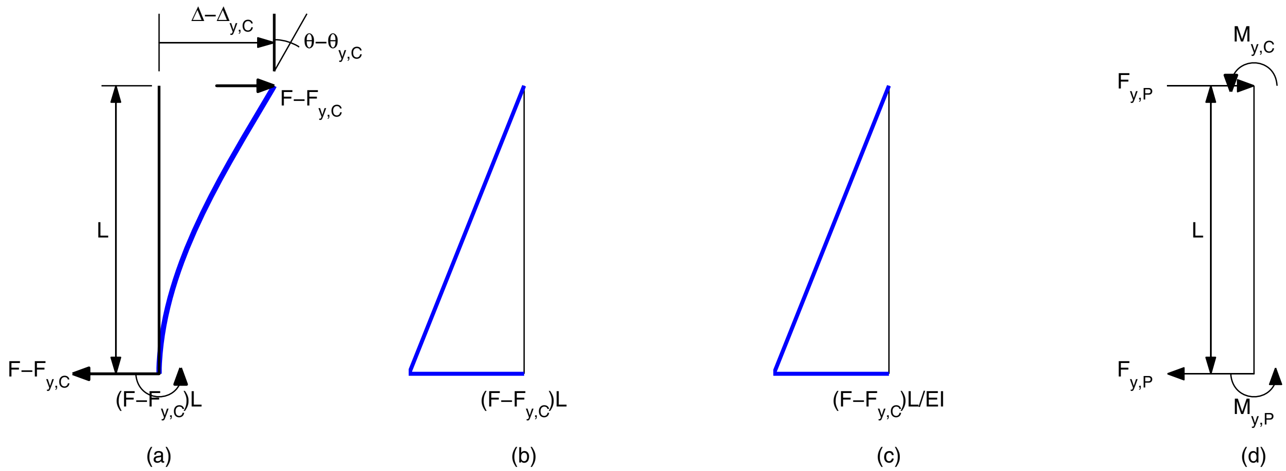

Δ−Δ y,C
θ−θ y,C
F−F y,C
L
F−F y,C
(F−F y,C)L
(a)
(F−F y,C)L
(b)
(F−F y,C)L/EI
(c)
M y,C
F y,P
L
F y,P
M y,P
(d)

Figure 15

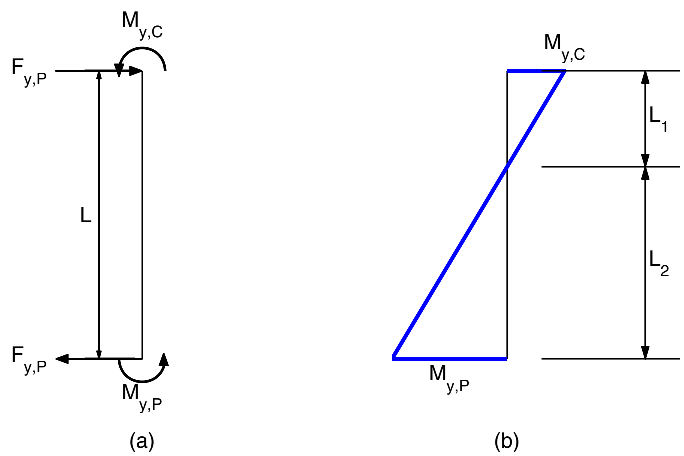

Table 1. Material strain limits in the MOTEMS.

Pile Type	Material	Hinge Location	Level 1	Level 2
Pre-stressed-concrete	Steel	In-Ground	$\varepsilon_p \le 0.005$ (Incremental)	$\varepsilon_p \le 0.04$ (Total)
		Pile/Deck	$\varepsilon_s \le 0.01$	$\varepsilon_s \le 0.05$
	Concrete	In-Ground	$\varepsilon_c \le 0.005$	$\varepsilon_c \le 0.008$
		Pile/Deck	$\varepsilon_c \le 0.005$	$\varepsilon_c \le 0.025$
Hollow-steel	Steel	In-Ground	$\varepsilon_s \le 0.008$	$\varepsilon_s \le 0.025$
		Pile/Deck	$\varepsilon_s \le 0.01$	$\varepsilon_s \le 0.05$